1158 *Inorg. Chem.* **2010**, *49*, 1158–1165
DOI: 10.1021/ic902077j

Inorganic Chemistry
Article

Porous Coordination Polymer with Flexibility Imparted by Coordinatively Changeable Lithium Ions on the Pore Surface

Lin-Hua Xie, Jian-Bin Lin, Xiao-Min Liu, Yu Wang, Wei-Xiong Zhang, Jie-Peng Zhang,* and Xiao-Ming Chen*

MOE Key Laboratory of Bioinorganic and Synthetic Chemistry, State Key Laboratory of Optoelectronic Materials, School of Chemistry and Chemical Engineering, Sun Yat-Sen University, Guangzhou 510275, China

Received October 21, 2009

Solvothermal reactions of equimolar zinc acetate, lithium acetate, and 1,3,5-benzenetricarboxylic acid (H_3btc) in different mixed solvents yielded isostructural three-dimensional frameworks [LiZn(btc)(cG)]·lG [cG and lG denote coordinated and lattice guests, respectively; cG = $(nmp)_{0.5}(H_2O)_{0.5}$, lG = $(EtOH)_{0.5}$ (**1a**); cG = H_2O, lG = EtOH (**1b**); nmp = *N*-methyl-2-pyrrolidone] with one-dimensional channels occupied by guest molecules and solvent-coordinated, extrusive Li^+ ions. Thermogravimetry analyses and powder X-ray diffraction measurements revealed that both **1a** and **1b** can lose all lattice and coordinated guests to form a desolvated phase [LiZn(btc)] (MCF-27, **1**) and almost retains the original framework structure. Gas adsorption measurements on **1** confirmed its permanent porosity but suggested a structural transformation from **1a**/**1b** to **1**. It is noteworthy that only **1a** can undergo a single-crystal to single-crystal (SCSC) transformation into **1** upon desolvation. The crystal structure of **1** revealed that the Li^+ ions were retracted into the channel walls via complementary coordination to the carboxylate oxygen atoms in the framework rather than being exposed on the pore surface. Single-crystal X-ray diffraction analyses were also performed for N_2- and CO_2-loaded samples of **1**, revealing that the framework remained unchanged when the gases were adsorbed. Although the gas molecules could not be modeled, the residue electrons inside the channels demonstrated that the retracted Li^+ ions still behave as the primary interacting site for CO_2 molecules. Nevertheless, solvent molecules such as H_2O can readily compete with the framework oxygen atom to retrieve the extrusive Li^+ ions, accompanying the reverse structural transformation, i.e., from **1** to **1a**/**1b**.

Introduction

In the past decade, porous coordination polymers (PCPs) have been extensively investigated because of their potential in gas storage, catalysis, separation, and many other fields.[1] Various combinations of a large number of metal ions and available organic ligands led to a large family of PCPs. As a new type of porous material, high internal surface area and stability are two important factors for PCPs. Up to now, many stable PCPs with permanent porosity have been successfully isolated, and some of them exhibit ultrahigh surface areas over 4000 m^2/g.[2] On the other hand, there is an important feature for PCPs that has seldom been found in traditional inorganic and carbon-based porous materials, namely, flexibility, which refers to the fact that some frameworks are capable of changing their internal structures as responses to external stimuli, such as temperature, light, pressure, and guests. It is believed that these kinds of PCPs would be a new class of advanced materials for selectivity recognition, increased storage, facile delivery, sensor, and switch. So far, however, reported dynamic PCPs are still rare, and the rational design and synthesis of these kinds of environmentally responsive materials remain a challenge.[3−12]

*To whom correspondence should be addressed. E-mail: zhangjp7@mail.sysu.edu.cn (J.-P.Z.), cxm@mail.sysu.edu.cn (X.-M.C.).

(1) (a) Férey, G. *Chem. Soc. Rev.* **2008**, *37*, 191–214. (b) Kitagawa, S.; Kitaura, R.; Noro, S. *Angew. Chem., Int. Ed.* **2004**, *43*, 2334–2375. (c) Yaghi, O. M.; O'Keeffe, M.; Ockwig, N. W.; Chae, H. K.; Eddaoudi, M.; Kim, J. *Nature* **2003**, *423*, 705–714. (d) Dinca, M.; Long, J. R. *Angew. Chem., Int. Ed.* **2008**, *47*, 6766–6779. (e) Morris, R. E.; Wheatley, P. S. *Angew. Chem., Int. Ed.* **2008**, *47*, 4966–4981.

(2) (a) Koh, K.; Wong-Foy, A. G.; Matzger, A. J. *J. Am. Chem. Soc.* **2009**, *131*, 4184–4185. (b) Koh, K.; Wong-Foy, A. G.; Matzger, A. J. *Angew. Chem., Int. Ed.* **2008**, *47*, 677–680. (c) Férey, G.; Mellot-Draznieks, C.; Serre, C.; Millange, F.; Dutour, J.; Surble, S.; Margiolaki, I. *Science* **2005**, *309*, 2040–2042. (d) Chae, H. K.; Siberio-Perez, D. Y.; Kim, J.; Go, Y.; Eddaoudi, M.; Matzger, A. J.; O'Keeffe, M.; Yaghi, O. M. *Nature* **2004**, *427*, 523–527. (e) Zhao, D.; Yuan, D. Q.; Su, D. F.; Zhou, H. C. *J. Am. Chem. Soc.* **2009**, *131*, 9186–9188.

(3) Maji, T. K.; Matsuda, R.; Kitagawa, S. *Nat. Mater.* **2007**, *6*, 142–148.

(4) Tanaka, D.; Nakagawa, K.; Higuchi, M.; Horike, S.; Kubota, Y.; Kobayashi, L. C.; Takata, M.; Kitagawa, S. *Angew. Chem., Int. Ed.* **2008**, *47*, 3914–3918.

(5) Choi, H. J.; Dinca, M.; Long, J. R. *J. Am. Chem. Soc.* **2008**, *130*, 7848–7850.

(6) Llewellyn, P. L.; Maurin, G.; Devic, T.; Loera-Serna, S.; Rosenbach, N.; Serre, C.; Bourrelly, S.; Horcajada, P.; Filinchuk, Y.; Férey, G. *J. Am. Chem. Soc.* **2008**, *130*, 12808–12814.

(7) Serre, C.; Mellot-Draznieks, C.; Surble, S.; Audebrand, N.; Filinchuk, Y.; Férey, G. *Science* **2007**, *315*, 1828–1831.

(8) Chandler, B. D.; Enright, G. D.; Udachin, K. A.; Pawsey, S.; Ripmeester, J. A.; Cramb, D. T.; Shimizu, G. K. H. *Nat. Mater.* **2008**, *7*, 229–235.

(9) Halder, G. J.; Kepert, C. J.; Moubaraki, B.; Murray, K. S.; Cashion, J. D. *Science* **2002**, *298*, 1762–1765.

 Published on Web 01/05/2010

Additionally, many recent works have been devoted to PCP systems containing coordinatively unsaturated metal centers (UMCs) to enhance the interaction between the host frameworks and adsorbates, especially hydrogen.[13] However, it is difficult to realize and characterize UMCs in these systems because removal of the coordinated solvent frequently leads to corruption of the framework or transformation of the metal coordination geometry that even the framework retains.[14] It is meaningful to determine the crystal structure of the desolvated phase to confirm the final coordination status of the metal ion. With consideration of their gravimetric gas storage capacity, some theoretical studies had been performed on models of PCPs doped by the lightest metal lithium atoms exposed on their internal surface, revealing a significant improvement of the H_2 uptake capacity.[15] Experimentally, many investigations have also been carried out to immobilize coordinatively unsaturated Li^+ ions on the pore surface of PCPs.[16−20] Eddaoudi and co-workers reported that the extra-framework cations (K^+ or dimethylammonium) of zeolite-like PCPs were exchangeable with Li^+ as aqua complexes. Nevertheless, it was found that the removal of aqua ligands of Li^+ would result in degradation of the frameworks.[16] Hupp and co-workers reported that interwoven PCPs doped with Li^+ exhibited enhanced H_2 uptake, but detailed investigations revealed that the enhanced H_2 uptake resulted from displacement of interwoven frameworks rather than exposed Li^+ because more extensive Li^+ doping decreased the H_2 loading.[17] Hartmann and co-workers reported that a MIL-53(Al) structural analogue with a ligand containing a pendant hydroxyl group could be lithium(+) alkoxide modified. Both the H_2 uptake and isosteric heat of H_2 adsorption increased after such a modification. However, because the framework undergoes a slow temperature-induced transformation from the high-temperature phase to the low-temperature phase (decreased pore volume) upon cooling to perform the adsorption experiment, it was believed that the observed increase of H_2 uptake was not caused exclusively by the Li^+ doping, and separation of the pure effect of Li^+ doping from the effect of the phase transformation remained to be studied.[18] Champness's and Schröder's groups showed that dimethylammonium cations in an indium-based PCP could be exchanged with Li^+ ions. After exchange, the H_2 uptake was enhanced. However, it was believed that Li^+ ions in the PCP were not accessible to H_2 molecules because a lower isosteric heat of H_2 adsorption was found for the exchanged material, even though complete desolvation of the Li^+ ions was confirmed.[19a] Recently, they reported that piperazinium dications in an indium-based PCP could be exchanged with Li^+ ions. After activation of the exchanged phase, an enhanced H_2 adsorption capacity coupled to an increased isosteric heat of H_2 adsorption was observed. According to these findings, the Li^+ ions were supposed to be partially exposed after removal of the coordinated guest, although the precise structure of the desolvated phase has not been determined.[19b] All of these reports reveal that the coordination status of the Li^+ ions in the activated framework is difficult to identify but significant for elucidation of the relationship between their structures and sorption performances. Actually, there is no report dealing with the crystal structural characterization of coordinatively unsaturated Li^+ ions in PCPs.

Scheme 1. Schematic Representation of Structural Transformations for **1**[a]

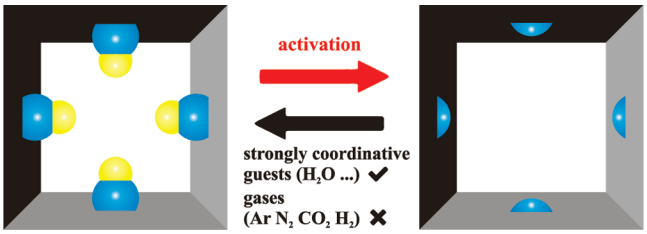

[a] Sky-blue and yellow spheres represent Li^+ ions on the pore surface of the framework and coordinated guests, respectively.

In this contribution, we present a new, porous, heterometallic carboxylate framework [LiZn(btc)] (MCF-27, **1**; H_3-btc = 1,3,5-benzenetricarboxylic acid), which can be obtained by thermal activation of its as-synthesized, solvated forms [LiZn(btc)(cG)]·lG [cG and lG denote coordinated guests and lattice guests, respectively; cG = $(nmp)_{0.5}(H_2O)_{0.5}$, lG = $(EtOH)_{0.5}$ (**1a**); cG = H_2O, lG = EtOH (**1b**); nmp = *N*-methyl-2-pyrrolidone] with solvent-bound Li^+ ions extrusive into the pores as potentially useful UMCs. In addition to thermogravimetry (TG) analyses, powder X-ray diffraction (PXRD) measurements, and gas sorption measurements, single-crystal structure determinations for guest-free and gas-loaded **1** were also conducted to investigate the coordination status of the Li^+ ions and flexibility of the framework. It is revealed that dramatic environmental changes of the Li^+ ion take place when all of the guests are removed, and after the transformation, the Li^+ ions distinctively respond to the stimulations of different guests (Scheme 1).

Experimental Section

Materials and General Methods. Solvents and reagents were obtained from commercial sources and used as received.

(10) Kondo, A.; Noguchi, H.; Ohnishi, S.; Kajiro, H.; Tohdoh, A.; Hattori, Y.; Xu, W. C.; Tanaka, H.; Kanoh, H.; Kaneko, K. *Nano Lett.* **2006**, *6*, 2581–2584.
(11) Zhang, J.-P.; Chen, X.-M. *J. Am. Chem. Soc.* **2008**, *130*, 6010–6017.
(12) Ma, S. Q.; Sun, D. F.; Yuan, D. Q.; Wang, X. S.; Zhou, H. C. *J. Am. Chem. Soc.* **2009**, *131*, 6445–6451.
(13) (a) Chen, B. L.; Ockwig, N. W.; Millward, A. R.; Contreras, D. S.; Yaghi, O. M. *Angew. Chem., Int. Ed.* **2005**, *44*, 4745–4749. (b) Ma, S. Q.; Zhou, H. C. *J. Am. Chem. Soc.* **2006**, *128*, 11734–11735. (c) Forster, P. M.; Eckert, J.; Heiken, B. D.; Parise, J. B.; Yoon, J. W.; Jhung, S. H.; Chang, J. S.; Cheetham, A. K. *J. Am. Chem. Soc.* **2006**, *128*, 16846–16850. (d) Dinca, M.; Dailly, A.; Liu, Y.; Brown, C. M.; Neumann, D. A.; Long, J. R. *J. Am. Chem. Soc.* **2006**, *128*, 16876–16883. (e) Lee, Y. G.; Moon, H. R.; Cheon, Y. E.; Suh, M. P. *Angew. Chem., Int. Ed.* **2008**, *47*, 7741–7745. (f) Wu, H.; Zhou, W.; Yildirim, T. *J. Am. Chem. Soc.* **2009**, *131*, 4995–5000.
(14) (a) Chen, C. L.; Goforth, A. M.; Smith, M. D.; Su, C. Y.; zur Loye, H. C. *Angew. Chem., Int. Ed.* **2005**, *44*, 6673–6677. (b) Suh, M. P.; Cheon, Y. E.; Lee, E. Y. *Chem.—Eur. J.* **2007**, *13*, 4208–4215. (c) Sakamoto, H.; Matsuda, R.; Bureekaew, S.; Tanaka, D.; Kitagawa, S. *Chem.—Eur. J.* **2009**, *15*, 4985–4989.
(15) (a) Han, S. S.; Goddard, W. A. *J. Am. Chem. Soc.* **2007**, *129*, 8422–8423. (b) Blomqvist, A.; Araujo, C. M.; Srepusharawoot, P.; Ahuja, R. *Proc. Natl. Acad. Sci. U.S.A.* **2007**, *104*, 20173–20176. (c) Klontzas, E.; Mavrandonakis, A.; Tylianakis, E.; Froudakis, G. E. *Nano Lett.* **2008**, *8*, 1572–1576.
(16) (a) Sava, D. F.; Kravtsov, V. C.; Nouar, F.; Wojtas, L.; Eubank, J. F.; Eddaoudi, M. *J. Am. Chem. Soc.* **2008**, *130*, 3768–3770. (b) Nouar, F.; Eckert, J.; Eubank, J. F.; Forster, P.; Eddaoudi, M. *J. Am. Chem. Soc.* **2009**, *131*, 2864–2870.
(17) (a) Mulfort, K. L.; Hupp, J. T. *J. Am. Chem. Soc.* **2007**, *129*, 9604–9605. (b) Mulfort, K. L.; Hupp, J. T. *Inorg. Chem.* **2008**, *47*, 7936–7938. (c) Mulfort, K. L.; Wilson, T. M.; Wasielewski, M. R.; Hupp, J. T. *Langmuir* **2009**, *25*, 503–508.
(18) Himsl, D.; Wallacher, D.; Hartmann, M. *Angew. Chem., Int. Ed.* **2009**, *48*, 4639–4642.
(19) (a) Yang, S. H.; Lin, X.; Blake, A. J.; Thomas, K. M.; Hubberstey, P.; Champness, N. R.; Schröder, M. *Chem. Commun.* **2008**, 6108–6110. (b) Yang, S. H.; Lin, X.; Blake, A. J.; Walker, G. S.; Hubberstey, P.; Champness, N. R.; Schröder, M. *Nat. Chem.* **2009**, *1*, 487–493.
(20) Dinca, M.; Long, J. R. *J. Am. Chem. Soc.* **2007**, *129*, 11172–11176.

Table 1. Crystal Data and Structure Refinements for **1a**, **1b**, **1**, and N_2- and CO_2-Loaded **1**

	1a	**1b**	**1**	N_2-loaded **1**	CO_2-loaded **1**
empirical formula	$LiZnC_{12.5}H_{11.5}N_{0.5}O_{7.5}$	$LiZnC_{11}H_{11}O_8$	$LiZnC_9H_3O_6$	$LiZnC_9H_3O_6$	$LiZnC_9H_3O_6$
M	361.03	343.51	279.42	279.42	279.42
temperature (K)	103	293	293	103	195
cryst syst	tetragonal	tetragonal	tetragonal	tetragonal	tetragonal
space group	$P4_12_12$	$P4_12_12$	$P4_12_12$	$P4_12_12$	$P4_12_12$
a (Å)	16.592(2)	16.6332(9)	16.3463(10)	16.3514(6)	16.3136(1)
c (Å)	10.856(3)	10.7833(11)	11.2519(13)	11.2764(8)	11.3049(2)
V (Å^3)	2988.5(10)	2983.3(4)	3006.5(4)	3015.0(3)	3008.61(6)
Z	8	8	8	8	8
D_{calc} (g/cm^3)	1.605	1.530	1.235	1.235	1.235
μ (mm^{-1})	1.678	1.677	1.640	1.640	1.640
reflns collected	14 311	9855	13 561	12 084	11 190
indep reflns	3053	3057	3074	3038	2381
θ range (deg)	2.24−26.37	1.73−26.37	2.49−26.37	1.76−26.37	3.83−62.45
GOF	1.069	0.994	1.093	1.060	1.338
R1 [$I > 2\sigma(I)$][a]	0.0483	0.0470	0.0366	0.0337	0.0624
wR2 (all data)[b]	0.1359	0.1074	0.0971	0.0805	0.2129
Flack parameter	0.03(2)	0.05(2)	−0.01(2)	−0.002(16)	0.05(8)
$\Delta\rho_{max/min}$ (e/Å^3)	0.736/−0.871	0.549/−0.320	0.667/−0.270	0.385/−0.418	1.264/−1.512

[a] $R1 = \sum||F_o| - |F_c||/\sum|F_o|$. [b] $wR2 = [\sum w(F_o^2 - F_c^2)^2/\sum w(F_o^2)^2]^{1/2}$.

Elemental analyses were performed on a Perkin-Elmer 240 elemental analyzer (C, H, and N). IR spectra were recorded in the range of 400−4000 cm^{-1} on a Bruker TENSOR 27 Fourier transform IR (FT-IR) spectrophotometer using KBr pellets. TG analyses were performed on a Netzsch TG 209 instrument in flowing N_2 with a heating rate of 10 °C/min. PXRD measurements were performed on a Bruker D8 ADVANCE X-ray diffractometer with Cu Kα radiation. For variable-temperature PXRD (VTPXRD) measurements, the diffraction patterns for different temperatures were recorded after the sample had stayed at the respective temperature for 30 min in a N_2 atmosphere. Ar, N_2, and H_2 sorption measurements were performed using a Micromeritics ASAP 2020 instrument. CO_2 sorption measurement was performed with a Belsorp-Max automatic volumetric adsorption apparatus.

Syntheses of $[LiZn(btc)(nmp)_{0.5}(H_2O)_{0.5}]\cdot 0.5EtOH$ (1a) and $[LiZn(btc)(H_2O)]\cdot EtOH$ (1b). $Zn(CH_3COO)_2\cdot 2H_2O$ (0.132 g, 0.6 mmol), $Li(CH_3COO)\cdot 2H_2O$ (0.062 g, 0.6 mmol), and H_3btc (0.147 g, 0.6 mmol) were added to a mixed solvent of nmp (6 mL) and anhydrous ethanol (18 mL) in a 40-mL Teflon-lined reactor. The resultant suspension was stirred for about 1 h, then sealed, and heated at 160 °C for 4 days. Block-shaped colorless crystals of **1a** were obtained in a yield of 0.176 g (81.2%). Anal. Calcd (%) for $LiZnC_{12.5}H_{11.5}N_{0.5}O_{7.5}$: C, 41.58; H, 3.21; N, 1.94. Found: C, 40.27; H, 3.24; N, 2.10. FT-IR (KBr pellet, cm^{-1}): 3421(m), 3072(w), 2968(w), 2939(w), 2877(w), 2501(w), 1627(s), 1566(s), 1544(s), 1438(s), 1367(s), 1110(m), 1041(w), 941(w), 883(w), 775(m), 725(m), 663(w), 580(w), 474(w).

Compound **1b** was synthesized in under conditions similar to those of **1a** except that the solvents were replaced by anhydrous ethanol (12 mL) and anhydrous methanol (12 mL), and the reaction temperature was 90 °C. Yield: 0.172 g, 83.5%. Anal. Calcd (%) for $LiZnC_{11}H_{11}O_8$: C, 38.46; H, 3.23. Found: C, 38.71; H, 3.34. FT-IR (KBr pellet, cm^{-1}): 3409(m), 1620(s), 1566(s), 1440(s), 1371(s), 1107(w), 1110(w), 941(w), 883(w), 819(w), 767(m), 725(m), 547(w), 466(w).

X-ray Crystallography. Single-crystal XRD data were collected on a Bruker Apex CCD area-detector diffractometer with Mo Kα monochromatic radiation or an Oxford Gemini S Ultra X-ray single-crystal diffractometer with Cu Kα monochromatic radiation. The single crystal of **1** was obtained by heating a single crystal of **1a** in a capillary at 280 °C under high vacuum for about 3 h and then sealed by fire (Figure S1 in the Supporting Information). The N_2- and CO_2-loaded single crystals of **1** were obtained from **1** in a capillary backfilled with N_2 or CO_2 and finally sealed by fire under a liquid-N_2 bath. The structures were solved by direct methods and refined by a full-matrix least-squares method on F^2 using the *SHELXTL* crystallographic software package. All hydrogen atoms were placed geometrically, and anisotropic thermal parameters were used to refine all non-hydrogen atoms. For N_2- and CO_2-loaded **1**, the gas molecules cannot be modeled; only the frameworks were refined. For **1a** and **1b**, disordered guest molecules cannot be modeled and were treated by the *SQUEEZE* routine,[21] and their amounts were determined by the TG results and elemental analyses. The crystal data and structure refinement results for these compounds are listed in Table 1.

Results and Discussion

Syntheses and Crystal Structures. 1a and **1b** were isolated by the solvothermal reaction of equimolar zinc acetate, lithium acetate, and a H_3btc ligand in different solvents. Mixed solvents were necessary for the syntheses of both compounds. Before solvothermal reactions, stirring of the heterogeneous solutions for a period of time was helpful for a high purity of both compounds, which was confirmed by their PXRD patterns (Figure S2 in the Supporting Information). It ought to be mentioned that when the sample of **1b** was exposed to the air for hours, several additional peaks appeared in its PXRD pattern compared with that of its as-synthesized sample (Figure S2e in the Supporting Information). Commonly, this kind of phenomenon can result from the loss of guests. However, the original PXRD pattern of **1b** cannot be recovered by immersion of the exposed sample in the mother liquor (Figure S2f in the Supporting Information). Thus, the structural transformation should not be caused by desolvation. Instead, the new phase possibly resulted from the interaction between the sample and moisture in the air.[22]

Single-crystal XRD reveals one Zn^{2+}, one Li^+, one btc^{3-} ligand, half of a water molecule, and half of a nmp molecule in the asymmetric unit of **1a**. The Zn^{2+} ion is coordinated by four carboxylate oxygen atoms (O1, O2, O3, and O6) from four btc^{3-} ligands in a distorted

(21) Spek, A. L. *J. Appl. Crystallogr.* **2003**, *36*, 7–13.
(22) Zhang, J.-P.; Ghosh, S. K.; Lin, J.-B.; Kitagawa, S. *Inorg. Chem.* **2009**, *48*, 7970–7976.

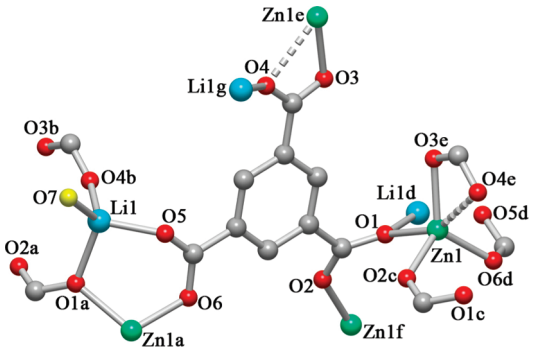

Figure 1. Coordination environment of **1a**. For clarity, all hydrogen atoms are omitted and only the coordinated oxygen atom (yellow) is shown for the coordinated solvent molecule. Symmetry codes: a, $-0.5+y, 0.5-x, 0.75+z$; b, $1-y, 1-x, 1.5-z$; c, $-0.5+y, 0.5-x, -0.25+z$; d, $0.5-y, 0.5+x, -0.75+z$; e, $1-y, 1-x, 0.5-z$; f, $0.5-y, 0.5+x, 0.25+z$; g, $1-y, 1-x, 1.5-z$.

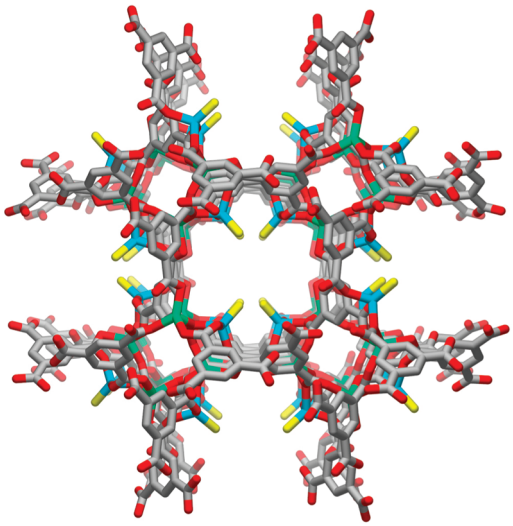

Figure 2. Perspective view of the coordination framework of **1a** along the *c* axis. Simplification and color codes follow those of Figure 1.

tetrahedral geometry with the Zn−O bond length in the range of 1.942(3)−2.055(3) Å and also weakly coordinated by another carboxylate oxygen atom [Zn1−O4 = 2.424(4) Å; Figure 1]. The Li^+ ion is coordinated by three carboxylate oxygen atoms (O1, O4, and O5) from three btc^{3-} ligands and one oxygen atom (O7) from the aqua or nmp ligand [Li−O = 1.864(12)−1.990(10) Å], which are statistically disordered at the same position with half-occupancy. The coordination geometry of Li^+ is a slightly distorted tetrahedron [O−Li−O = 101.3(5)−115.2(6)°]. The btc^{3-} ligand bridges four Zn^{2+} ions and three Li^+ ions by its six carboxylate oxygen atoms. Along the *c* axis, an alternate connection of Zn^{2+} and Li^+ ions by btc^{3-} carboxylates results in a 4_1 helical chain (Figure S3 in the Supporting Information). Such chains are interconnected with four neighboring equivalent chains via btc^{3-} ligands, giving rise to a three-dimensional (3D) structure (Figure 2). There are helical one-dimensional (1D) channels with diameters ranging from 5.8 to 6.3 Å running along the *c* axis, which exhibit 40.3% volume of the crystal.[21] These channels are occupied by the aqua and nmp solvents as well as disordered guest ethanol molecules. It is noteworthy that the Li^+ ions are extrusive into the channels, which suggests that they can potentially serve as UMCs after removal of the guests and coordinated molecules. **1b** is isostructural to **1a** except that all of the coordinated solvents in **1b** are water molecules. Note that both **1a** and **1b** are spontaneously resolved racemic conglomerates and crystallize in the chiral space group of $P4_12_12$ (No. 92) or $P4_32_12$ (No. 96).

Thermal Behaviors. To evaluate the thermal behaviors of **1a** and **1b**, TG analyses and VTPXRD measurements were conducted. For **1a**, the TG curve shows two steps of weight loss below 350 °C, followed by a plateau until 430 °C when the compound became to decompose (Figure S4 in the Supporting Information). The first weight loss between room temperature and 120 °C was 6.5%, corresponding to the departure of ethanol guests (calcd 6.4%). The 16.7% weight loss between 120 and 350 °C corresponds to the release of the coordinated water and nmp molecules (calcd 16.2%). The VTPXRD patterns for **1a** were collected from 30 to 380 °C under a N_2 atmosphere. Some peaks of its diffraction pattern were slightly shifted when the sample was heated at 140−220 °C (Figure S5 in the Supporting Information), which should result from the small distortion of the framework when the desolvated phase **1** was produced. Note that the peak intensities of the PXRD patterns became stronger when the temperature was gradually elevated. In the TG curve of **1b**, there is an abrupt weight loss of 13.8%, corresponding to the release of the ethanol guest molecules (calcd 13.4%) before 100 °C, followed by a gradual weight loss of 5.1% until 350 °C, corresponding to the removal of coordinated water molecules (calcd 5.2%; Figure S6 in the Supporting Information). The VTPXRD patterns show that there is an apparent structural rearrangement when the ethanol guest molecules were removed at 60 °C. However, all of the PXRD patterns above this temperature appear to be identical with that of **1** only with slight differences in the intensities of the peaks (Figure S7 in the Supporting Information). This fact implies that the cell parameters of the sample were basically maintained when the coordinated water molecules were gradually removed at higher temperatures because the TG results indicated the loss of coordinated water molecules at relatively high temperature above 100 °C.

Sorption Studies. To evaluate the porosity of **1**, gas sorption studies were conducted. The sample of guest-free **1** was obtained by heating **1a** at 280 °C for 8 h under a high vacuum. Ar (87 K), N_2 (77 K), and CO_2 (195 K) sorption measurements for **1** gave type I isotherms typical for microporous materials, and the uptakes around 1 atm are 271, 211, and 174 cm^3/g, respectively (Figure 3). The apparent Brunauer−Emmett−Teller and Langmuir surface areas of **1** calculated from the Ar adsorption isotherm are 725 and 962 m^2/g, respectively. Assuming that the gases are micropore filling in the channels of desolvated **1a** as the liquid (densities for liquid Ar, N_2, and CO_2: 1.40, 0.808, and 1.101 g/cm^3), the theoretically saturated uptakes of the three types of gases can be calculated as 255, 210, and 182 cm^3/g, respectively. Commonly, the measured uptakes should be less than the calculated ones, especially for guest molecules with large size and polarity (dipole, quadrupole, etc.) because of the preferred orientation of the guest molecules and space incommensurateness. In other words, Ar sorption

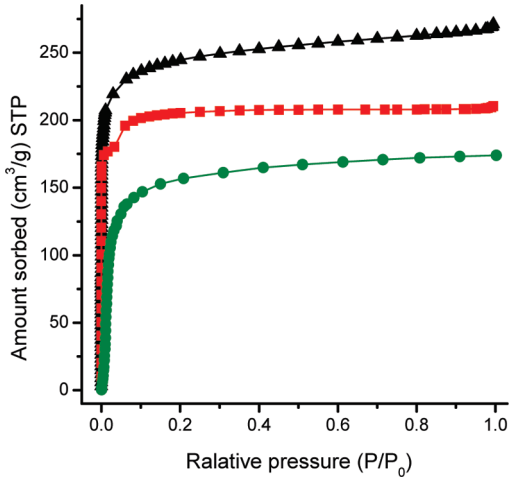

Figure 3. Adsorption isotherms of Ar (black), N_2 (red), and CO_2 (green) for **1** measured at 87, 77, and 195 K, respectively.

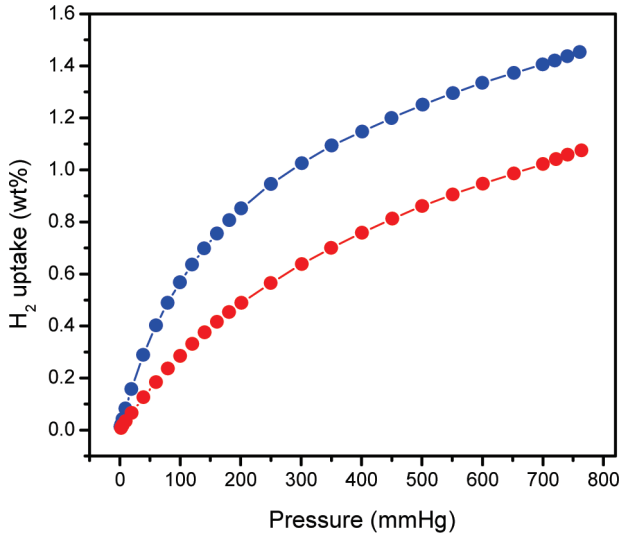

Figure 4. H_2 adsorption isotherms for **1** recorded at 77 K (blue) and 87 K (red).

measurement should generally give the most reliable pore characteristic among the selected gases used in this study. One may notice that the measured uptakes are very close to the predicted ones. Especially, the measured Ar uptake is obviously higher than the predicted value. The excessive adsorption of **1** compared to the predicted value implies that the coordination framework of **1a** is slightly expanded after the removal of all coordinated solvents and guests.

H_2 adsorption experiments were also conducted for **1** at 77 and 87 K, which show 163 and 120 cm^3/g uptakes around 1 atm, respectively (Figure 4). By fitting of the Langmuir−Freundlich equation to the isotherms, the saturated H_2 uptake for **1** is estimated to be 235 cm^3/g. Virial analysis[23] of the H_2 adsorption isotherms revealed that the isosteric heat of adsorption of **1** at zero surface coverage is 5.9 kJ/mol and slightly decreases as the H_2 uptake increases (Figure S12 in the Supporting Information). This value of the isosteric heat of adsorption is comparable to that of MOF-5 (5.2 kJ/mol) but apparently lower than that of some PCPs containing UMCs.[23]

Single-Crystal to Single-Crystal (SCSC) Transformation. To interpret the results of adsorption experiments, it is necessary to obtain the precise structure of **1**. Inspired by its VTPXRD patterns, we attempted to perform SCSC transformation experiments for single crystals of **1a**. It was found that the single crystallinity of the crystals of **1a** was retained after being heated at 280 °C for 3 h under a high vacuum to remove the uncoordinated and coordinated solvents. In contrast, the SCSC transformation experiment from **1b** to **1** was unsuccessful. Single crystals of **1b** easily crack after heating. Its structural rearrangement induced by the loss of ethanol guests may be responsible for the friable character, whereas the framework of **1a** is unchanged when its ethanol guests are removed, as demonstrated by the VTPXRD patterns.

Single-crystal XRD of **1** revealed that the crystal retains the tetragonal crystal system and the original space group, with the unit cell parameters being slightly changed. The *a* and *b* axes are shortened from 16.592(2) to 16.3463(10) Å, while the *c* axis is lengthened from 10.856(3) to 11.2519(13) Å. There are one Zn^{2+}, one Li^+, and one btc^{3-} ligand in the asymmetric unit of **1**. The Zn^{2+} ion is also coordinated by four carboxylate oxygen atoms [O1, O2, O3, and O5; Zn−O = 1.901(2)−2.040(2) Å] in a distorted tetrahedral geometry and weakly coordinated by another oxygen O6 atom [2.669(3) Å]. However, the Li^+ ion is now coordinated by four carboxylate oxygen atoms [O1, O4, O5, and O6; 1.855(6)−2.025(7) Å] from four btc^{3-} ligands in a more distorted tetrahedral geometry [O−Li−O = 83.9(2)−137.8(4)°; Figure S8 in the Supporting Information]. Compared with the structure of **1a**, it is not difficult to rationalize the structural transformation process. When the coordinated guest (O7) is removed, Li1 and O6 approach each other to form a new coordination bond. Meanwhile, O4, O5, and O6 either approach or depart from Zn1, resulting in the formation or cleavage of coordination bonds. O1, O2, and O3 are also slightly shifted to adapt the new coordination geometry of the metal atoms (Figure 5). In short, the Li^+ ion is shifted into a position of lower potential when the coordinated solvent is removed rather than being exposed on the pore surface (Figure 6), although the framework seems to be almost unchanged during the transformation according to the PXRD patterns. This rationalization of the structural change in the SCSC transformation from **1a** to **1** is in accordance with our previous observation of a "carboxylate shift" around metal centers in the SCSC transformation of dehydration of a 3D chiral cadmium(II) dicarboxylate coordination polymer.[24] These results reveal that it is more appropriate to regard the Li^+ ion as coordinatively changeable rather than coordinatively unsaturated. To our best knowledge, this is the first time that the removal of a coordinated solvent on a Li^+ ion is structurally characterized, which is fundamental for the investigations on PCPs with Li doping strategies.

(23) Chen, B.; Zhao, X.; Putkham, A.; Hong, K.; Lobkovsky, E. B.; Hurtado, E. J.; Fletcher, A. J.; Thomas, K. M. *J. Am. Chem. Soc.* **2008**, *130*, 6411−6423 and references cited therein.

(24) Xue, D.-X.; Zhang, W.-X.; Chen, X.-M.; Wang, H.-Z. *Chem. Commun.* **2008**, 1551–1553.

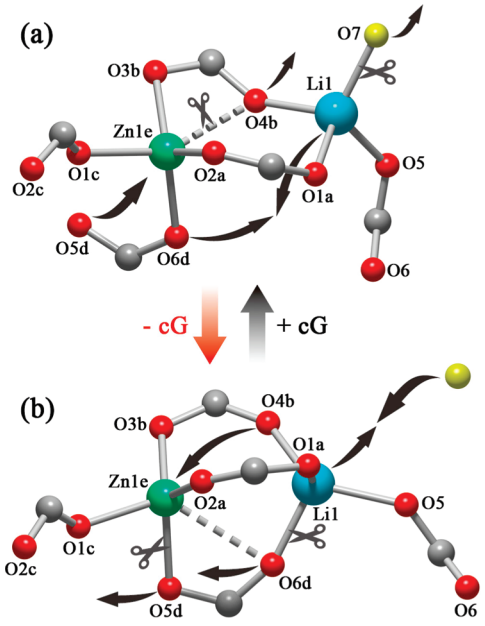

Figure 5. Coordination environments of the metal atoms in **1a** (a) and **1** (b). Simplification and color codes follow those in Figure 1. Symmetry codes: a, $-0.5+y, 0.5-x, 0.75+z$; b, $1-y, 1-x, 1.5-z$; c, $x, y, 1+z$; d, $0.5-y, 0.5+x, 0.25+z$; e, $x, y, 1+z$.

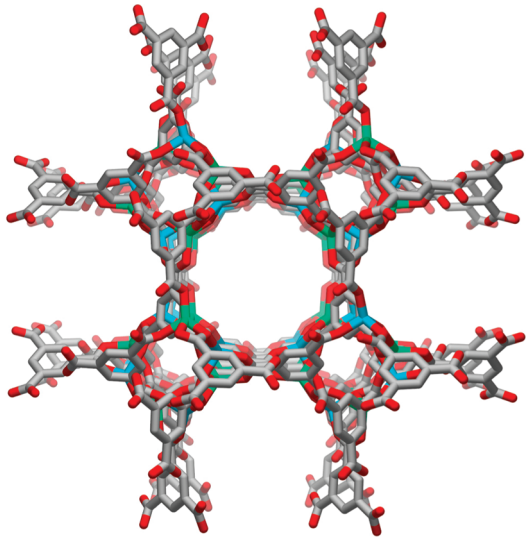

Figure 6. Perspective view of the framework of **1** along the *c* axis. Simplification and color codes follow those of Figure 1.

According to the SCSC studies, the structure of **1** may be regarded as the accurate structure of the activated sample of **1a** for the gas adsorption experiments. The channels of **1** along the *c* axis are close to being linear in spite of their helical nature (Figure S8 in the Supporting Information). The diameters of the channel sections are in the range of 7.1−7.3 Å; the volume for the channels corresponds to 45.3% of the structure;[21] the calculated density for the porous framework is 1.235 g/cm^3. With these results, calculated saturated gas adsorption amounts of **1** can be obtained. For Ar, this amount is 288 cm^3/g, close to the obtained value 271 cm^3/g (94%). The calculated values for N_2 and CO_2 are 237 and 206 cm^3/g, respectively, slightly higher than the experimentally obtained values of 211 cm^3/g (89%) and 174 cm^3/g (84%). These data imply that the adsorbed N_2 and CO_2 molecules are not ideally in their liquid status like the adsorbed inert Ar molecules are. The small Ar molecules are spherical and without a quadrupole, thus more effectively occupying the pores. In contrast, the adsorbed N_2 and CO_2 molecules may interact with the pore walls and occupy the pores with the preferred orientations, resulting in some wasted space. The calculated value of the micropore filling of liquid H_2 (density: 0.0708 g/cm^3) for **1** is 291 cm^3/g, also higher than the calculated saturated amount of 235 cm^3/g (81%) obtained by fitting of the isotherms with the Langmuir−Freundlich equation. Additionally, according to the structure of **1**, the Li^+ ions are four-coordinated with carboxylate oxygen atoms rather than exposed, providing the reason why the isosteric heat of adsorption for its H_2 uptake is relatively low.

Host−Guest Studies. Structural determination of the gas-loaded PCPs would be pivotal for the understanding of the adsorption mechanism by providing structural details of the guest inclusion phases. Such information at least illustrates whether the host framework is transformed or not after gas adsorption. Therefore, we also determined the structures of N_2- and CO_2-loaded single crystals of **1** at 103 and 195 K, respectively. Though the adsorbed gases cannot be modeled, it is unambiguous that the framework remained unchanged. The refinement for the diffraction data of N_2-loaded **1** revealed no significant peaks of electron density in the channels. However, there is an apparent decrease of the *R* factors for structural refinement after the *SQUEEZE* treatment (Table S1 in the Supporting Information). This fact suggests that the adsorbed N_2 molecules are highly disordered because of their very weak interaction with the framework. For CO_2-loaded **1**, there are many pronounced electron density peaks presented in the channels. The 3D electron density map ($F_o - F_c$) shows that the electron contribution of the adsorbed CO_2 molecules is primarily localized along the channel walls (Figure 7). The maximum of the electron density was in the vicinity of the Li^+ ion with a distance of 3.41 Å (Figure 8). This fact implies that the Li^+ ions still behave as the primary interacting sites for the adsorbed CO_2 molecules, although they only adopt distorted tetrahedral coordination geometries and were almost unexposed in **1**. This result is reminiscent of the situation of MOF-5 containing Zn^{2+} ions in similar coordination environments, in which the faces of ZnO_4 tetrahedra behave as the primary adsorption sites.[25]

Although the interactions between the Li^+ ions and the adsorbed gases are weak in **1**, the Li^+ ions may strongly interact with solvent molecules capable of coordination, such as water molecules. This deduction is supported by the fact that single crystallinity of **1** is immediately lost upon exposure to a moist atmosphere. The PXRD pattern of hydrated **1** reveals a slight structural rearrangement after hydration (Figure 9). The PXRD pattern of hydrated **1** matches well with that of the exposed sample of **1b** (Figure 9), which suggests that the framework of **1** was changed to that of **1b**, concomitant with a small

(25) Rowsell, J. L. C.; Spencer, E. C.; Eckert, J.; Howard, J. A. K.; Yaghi, O. M. *Science* **2005**, *309*, 1350–1354.

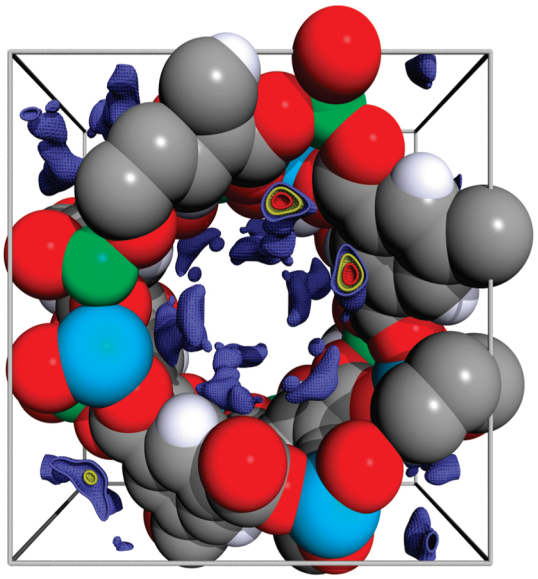

Figure 7. Perspective view of the 3D electron density map ($F_o - F_c$) in the unit cell of CO_2-loaded **1** along the *c* axis. Color codes for the contours (e/Å^3): blue, 0.6; yellow, 0.9; red, 1.2. Color codes for the atoms follow those of Figure 1.

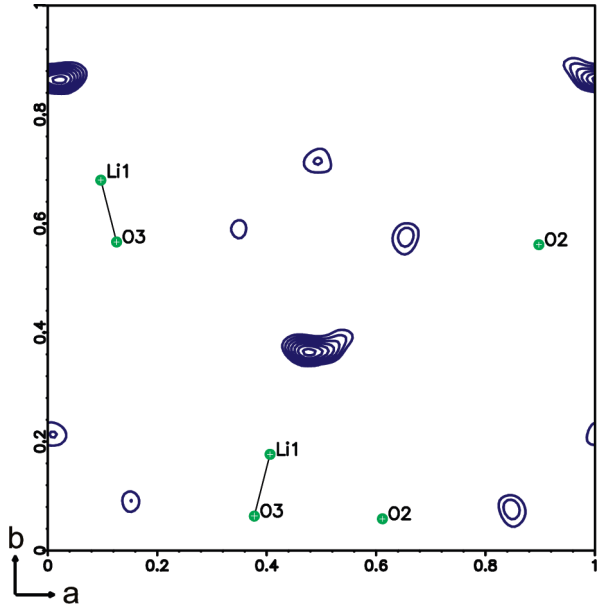

Figure 8. Section of the 3D electron density map ($F_o - F_c$) in the unit cell of CO_2-loaded **1** passing through a Li^+ ion. The contours are plotted with an interval of 0.1 e/Å^3.

amount of an unknown phase after exposure to a moist atmosphere. This finding also justifies our previous speculation that the structural transformation of **1b** after exposure to air resulted from the interaction between the sample and moisture. In other words, when stimulated by moisture, the Li^+ ions of **1** extrude back to coordinate water molecules. When coordinated solvents are removed, the Li^+ ions of **1a** are coordinated to the carboxylate oxygen atoms of the framework to compensate for their unstable coordination state; when being stimulated by moisture, the Li^+ ions of **1** are coordinated to water molecules and recover its previous coordination state (Figure 5). This type of coordination behavior for a

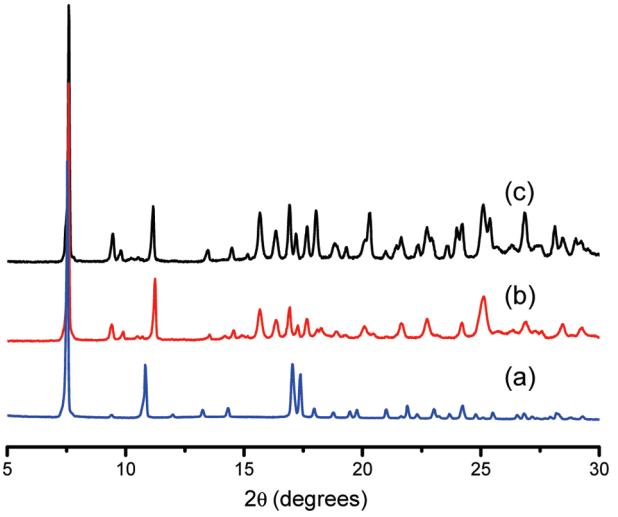

Figure 9. PXRD patterns for (a) an as-prepared sample of **1**, (b) a sample of **1** after exposure to air for minutes, and (c) a sample of **1b** after exposure to air for hours.

metal ion can be categorized as a kind of complementary coordination action, which has been scarcely observed in the literature.[14c] However, the occurrence of this type of behavior is dependent on the nature of the guests. As mentioned above, adsorption of gas did not lead to any significant change of the coordination state of the Li^+ ion. Therefore, it may be concluded that there is a competition between the guest and framework carboxylate oxygen atoms in coordination to the Li^+ ions.

Conclusion

We have described a porous 3D heterometallic carboxylate framework [LiZn(btc)], which represents a unique prototype for the study of the framework flexibility, coordinatively changeable Li^+ ions, and sorption property. At first glance, the material appears as a new PCP incorporated with coordinatively unsaturated Li^+ ions. The as-synthesized, solvated material [LiZn(btc)(cG)]·lG contains solvent-coordinated, extrusive Li^+ ions on the pore surface, and the framework retention after removal of the guest and coordinated solvent molecules was also confirmed by the TG and PXRD studies. However, such a rigid structure elucidation, which was commonly used in other similar cases, cannot satisfactorily explain the gas sorption data of the activated material [LiZn(btc)]. The measured H_2 adsorption enthalpy for the activated material [LiZn(btc)] is also lower than expected.

The single-crystal structures of the activated materials in guest-free and gas-loaded forms show that the Li^+ ions on the pore surface are actually retracted into the channel walls by complementary coordination to the framework carboxylate oxygen atoms rather than being exposed on the pore surface. The framework is not altered after N_2 or CO_2 adsorption. Although the binding strength is weak, the unexposed Li^+ ions still behave as the primary interacting sites of the porous framework, which can be revealed by the electron density distribution of the CO_2-adsorbed single crystal. For much strongly coordinative guests such as H_2O, the retracted Li^+ ions can readily extrude back to coordinate with the guest.

The direct structural information for the desolvated Li^+ ions would provide useful implication for the understanding

of Li-doping PCPs, where the coordination environments of the doped Li^+ ions on the pore surface are fundamental to the sorption mechanism. It is well-known that coordinatively unsaturated Li^+ ions are very energetically unstable as compared to other transition-metal ions such as Cu^{2+}. In contrast to zeolites, PCPs are usually not rigid enough to sustain the very unstable, coordinatively unsaturated Li^+ ions. Structural transformations must occur to lower the system energies after the introduction of coordinatively unsaturated Li^+ ions. Frequently, structural transformations result in the collapse of the PCPs. Even occasionally when PCPs are able to maintain their crystallinity after structural transformations, the Li^+ ions would very likely be transformed to certain unexposed environments. The dramatic changes in the coordination environments of the Li^+ ions may not cause a large structural variation of the crystal lattice and, hence, do not lead to critical changes in the PXRD patterns. Thus, PXRD patterns cannot serve as sufficient methods to justify the generation of UMCs, especially for Li^+ ions, whereas the unexposed Li^+ ions still behave as the primary interaction sites for guests compared to other places like organic ligands of the PCPs. This fact is possibly because of the relatively strong local electric fields around the inorganic moieties, which would have an influence on their gas (especially for polar molecules) sorption performances.

In summary, this work illustrates the critical importance of single-crystal structure determination for elucidation of the sorption properties of flexible PCPs, especially those showing coordinatively changeable Li^+ ions and weak interactions between the guests and host framework.

Acknowledgment. This work was supported by NSFC (Grants 20821001 and 20531070), the "973 Project" (Grant 2007CB815302), and the Chinese Ministry of Education (Grant 109125).

Supporting Information Available: PXRD, TG curves, additional structural figures, photograph of a single crystal of **1** sealed in a capillary, detail about the analysis of H_2 adsorption isotherms, and X-ray crystallographic files in CIF format. This material is available free of charge via the Internet at http://pubs.acs.org.